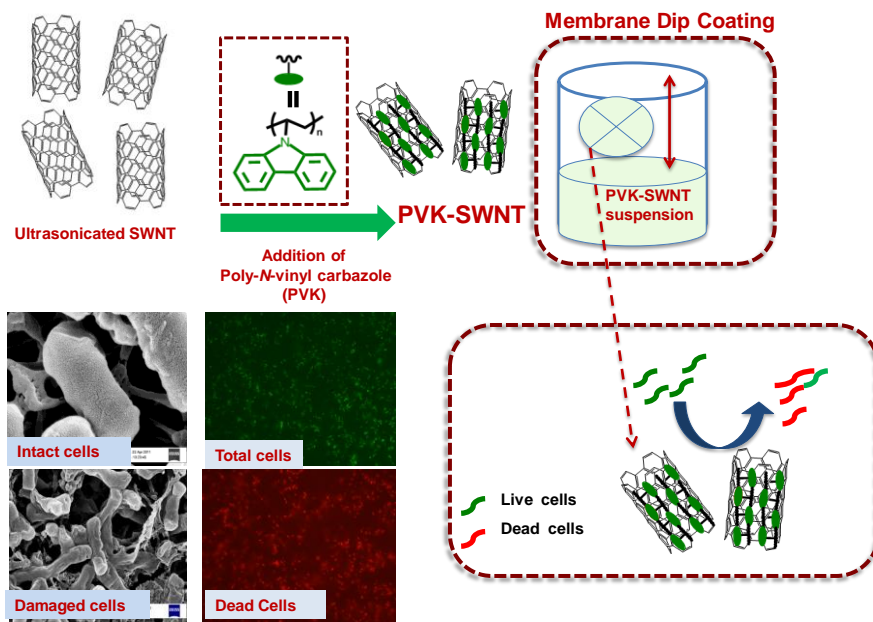


Highlights

Antimicrobial PVK:SWNT nanocomposite coated membrane for water purification: performance and toxicity testing

- Nitrocellulose membrane filters coated with PVK: SWNT (97:3 wt%) nanocomposite.
- High bacterial inactivation (~ 80-90%) on the filter surface was observed.
- High bacterial DNA concentration in the filtrate confirmed cell membrane damage.
- PVK-SWNT nanocomposites present minimal toxic effects to mammalian cells.



1 Antimicrobial PVK:SWNT nanocomposite coated
2 membrane for water purification: performance and
3 toxicity testing
4

5 *Farid Ahmed,^a Catherine M. Santos,^a Joey Mangadlao,^b Rigoberto Advincula,^b and Debora F.*
6 *Rodrigues^{a*}*

7
8 ^a Department of Civil and Environmental Engineering
9 University of Houston, Houston, TX 77204-5003 (USA)
10

11 ^b Department of Chemistry and Department of Chemical and Biomolecular Engineering
12 University of Houston, Houston, TX 772404-5003 USA
13

14
15
16 * Corresponding author: Department of Civil and Environmental Engineering
17 University of Houston
18 4800 Calhoun Rd, Houston, TX 77204
19 Tel.: +1 713 743 1495; Fax: +1 713 743 4260
20 E-mail: dfrigirodrigues@uh.edu
21

22 **Abstract**

23 This study demonstrated that coated nitrocellulose membranes with a nanocomposite containing
24 97% (wt%) of polyvinyl-*N*-carbazole (PVK) and 3% (wt%) of single-walled carbon nanotubes
25 (SWNTs) (97:3 wt% ratio PVK:SWNT) achieve similar or improved removal of bacteria when
26 compared with 100% SWNTs coated membranes. Membranes coated with the nanocomposite
27 exhibited significant antimicrobial activity towards Gram-positive and Gram-negative bacteria (~
28 80–90%); and presented a virus removal efficiency of ~2.5 logs. Bacterial cell membrane
29 damage was considered a possible mechanism of cellular inactivation since higher efflux of
30 intracellular material (Deoxyribonucleic acid, DNA) was quantified in the filtrate of PVK-
31 SWNT and SWNT membranes than in the filtrate of control membranes. To evaluate possible
32 application of these membrane filters for drinking water treatment, toxicity of PVK-SWNT was
33 tested against fibroblast cells. The results demonstrated that PVK-SWNT was non toxic to
34 fibroblast cells as opposed to pure SWNT (100%). These results suggest that it is possible to
35 synthesize antimicrobial nitrocellulose membranes coated with SWNT based nanocomposites for
36 drinking water treatment. Furthermore, membrane filters coated with the nanocomposite PVK-
37 SWNT (97:3 wt% ratio PVK:SWNT) will produce more suitable coated membranes for drinking
38 water than pure SWNTs coated membranes (100%), since the reduced load of SWNT in the
39 nanocomposite will reduce the use of costly and toxic SWNT nanomaterial on the membranes.

40

41

42 Keyword: Nitrocellulose membrane, Single-walled carbon nanotubes, nanocomposite, bacteria,
43 DNA, Cytotoxicity.

44

45 **1. Introduction**

46 Membrane separation systems are used for drinking water treatment because of their potential
47 to remove microorganisms (Hilal et al. 2004). The major issue of membrane operations is that
48 they are often affected by biofouling phenomena (*e.g.*, bacterial adhesion) on the membrane
49 surface (Khulbe et al. 2000). Membrane biofouling is initiated by bacterial adhesion and growth
50 on the membrane surface, which can eventually form a biofilm (Hilal et al. 2004). Hence,
51 developing membranes with anti-bacterial property is certainly an attractive solution. The most
52 common approach for developing anti-microbial membranes is the modification of commercial
53 membrane surfaces with polymeric materials containing silver nanoparticles (Aslan et al. 2010,
54 Liu et al. 2010). Similarly, carbon based nanomaterials, like single-walled carbon nanotubes
55 (SWNTs), have been reported to significantly reduce the bacterial and viral load in water due to
56 its anti-microbial properties (Kang et al. 2008, Kang et al. 2007, Kang et al. 2009, Brady-Estévez
57 et al. 2008). Apart from anti-microbial properties, incorporation of SWNT into membranes has
58 also been reported to improve membrane strength, thermal stability, and water flux (Peng et al.
59 2007). The use of SWNTs to coat membranes is, however, still limited by high cost and poor
60 dispersibility in aqueous solutions (Aslan et al. 2010, Arias and Yang 2009, Upadhyayula and
61 Gadhamshetty 2010). Though polymer nanocomposites have been used for surface modification
62 of membranes, SWNT incorporated in the polyvinyl-*N*-carbazole (PVK) polymer has not yet
63 been investigated for its application in water treatment. In our recent study with PVK-SWNT
64 nanocomposite in suspension and immobilized on solid surfaces, we demonstrated significant
65 antimicrobial effects against both Gram-positive and Gram-negative bacteria (Ahmed et al.
66 2012). PVK was selected as a base polymer because of its multiple aromatic groups that facilitate
67 π - π interaction with carbon-based nanomaterials, making it a more compatible polymer with

68 SWNT. Besides, PVK possesses excellent thermal, mechanical, and biocompatible properties
69 and is easy and economical to prepare (Guimard et al. 2007, Ahuja et al. 2007). Furthermore, the
70 ratio of SWNT in the PVK-SWNT (97:3 wt% ratio PVK: SWNT) nanocomposite reduces the
71 use of costly SWNT in the membrane preparation while showing excellent dispersion of SWNT
72 in aqueous solution in the presence of PVK (Cui et al. 2011).

73 In this study, we investigated the antimicrobial properties of nitrocellulose membrane
74 filters coated with PVK-SWNT (97:3 wt% ratios, PVK: SWNT). Highly purified and well
75 characterized SWNT was used to synthesize the PVK-SWNT nanocomposite. Membrane
76 surfaces were dip coated in PVK-SWNT suspension to create a film of PVK with a 3 wt%
77 SWNT load. Antibacterial and virus removal properties of the membranes coated with PVK-
78 SWNT was investigated with Gram-positive (*Bacillus subtilis*), Gram-negative (*Escherichia*
79 *coli*) bacteria and the model virus MS2. Cytotoxicity of PVK-SWNT nanocomposite was
80 investigated with mammalian fibroblast cells to assess suitability of this nanocomposite for
81 drinking water treatment.

82

83 **2. Materials and Methods**

84 *2.1 Single-walled carbon nanotubes preparation*

85 Single-walled carbon nanotubes (SWNTs) were purchased from Cheap Tubes Inc. (Vermont,
86 US). The results of the characterization of the SWNT are provided in the Supporting Information
87 (Table S1-S2, Figure S1). Prior to use, further purification of SWNT was done by heat treatment
88 at 200⁰C for 6 hours. The SWNT suspension was prepared in deionized water (DI) (1 mg/ml)
89 according to previously published methods (Rodrigues and Elimelech 2010). Briefly, SWNT was
90 dispersed in DI water through 3 cycles of sonication for 1 h.

91 2.2. Preparation of PVK and PVK-SWNT nanocomposite

92 The PVK-SWNT (97:3 wt% ratio PVK:SWNT) was prepared according to previously reported
93 procedure (Ahmed et al. 2012, Cui et al. 2011). Briefly, separate suspensions of 1mg/ml of
94 SWNT and PVK (Sigma Aldrich Chemicals, USA) were prepared by ultrasonication with N-
95 cyclohexyl-2-pyrrolidone (CHP). Later, 0.15 ml of the CHP-SWNT solution was added to 4.85
96 ml of CHP-PVK solution. The mixture was centrifuged (4400 rpm, 1h) and the pellet of PVK-
97 SWNT was washed with DI water and resuspended by Ultrasonication, which furnished a well
98 dispersed suspension of PVK-SWNT (1 mg/ml) in DI water. This procedure yielded a 97:3
99 weight ratio of well-dispersed PVK-SWNT mixture. The 97:3 (wt%) ratio of PVK and SWNT
100 was selected for this nanocomposite based on our previous study, which demonstrated that at
101 this particular ratio SWNT remains highly dispersed and stable for an extended period of time
102 (Cui et al. 2011). A PVK only suspension was prepared by dissolving PVK in water (1mg/ml)
103 followed by 1 h ultrasonication.

104 2.3. Coating of the filter membranes

105 Nitrocellulose membrane filters (0.45 μm , Milipore USA) were dip-coated with PVK
106 (1mg/ml), SWNT (1mg/ml) and PVK-SWNT (1 mg/ml) suspensions in DI water. Briefly, each
107 filter membrane was placed into a small petri dish containing 5 ml of the sample suspension to
108 cover the filter membrane completely. After 30 minutes of impregnation, the filter membranes
109 were carefully removed and dried overnight in a vacuum oven. Bare nitocellulose membranes
110 were used as controls. Characterization of PVK, SWNT, and PVK-SWNT suspensions and
111 coated membrane filters were conducted according to procedure described in our previous work
112 (Ahmed et al. 2012, Cui et al. 2011).

113 2.4. Bacterial Culture

114 Freshly prepared suspensions of *Escherichia coli* MG 1655 (*E. coli*) and *Bacillus subtilis*-
115 102 (*B. subtilis*) were used for all experiments in this study. In order to prepare fresh
116 suspensions, single isolated colonies of *E. coli* and *B. subtilis* were inoculated in 5 ml of Tryptic
117 Soya Broth (TSB) (Oxoid, England) and incubated overnight at 35 °C and 200 rpm (INNOVA
118 44, New Brunswick Scientific Co, USA). The bacterial culture was centrifuged at 10,000 rpm for
119 10 minutes. To remove any residual growth medium, cells were washed twice and re-suspended
120 in phosphate buffer solution (PBS, 0.01M, pH=7.4) (Fisher Scientific, USA). The bacterial
121 suspension was adjusted to give an optical density (OD) of 0.5 at 600 nm, which corresponds to
122 a cell concentration of $\sim 10^7$ colony forming units (CFU)/ml.

123 2.5. Bacterial Cell Filtration

124 All the filtration apparatus were sterilized prior to use. The prepared membrane filters were
125 washed for 15 min with ethanol (70%) and air dried for 24 h in a biological safety cabinet
126 (LABGARD, NuAire Inc, USA) under laminar flow to evaporate any residual ethanol. All the
127 filtration assays were conducted under a constant permeation rate ($\sim 57 \text{ L m}^{-2} \text{ h}^{-1}$) using a
128 peristaltic pump (Cole-Parmer, USA). The filtration experiment set up consisted of all glass
129 filtration apparatus with 47 mm stainless steel screen (Milipore, USA). The mode of filtrations
130 was dead-end. Prior to each filtration experiment, the filter surfaces were preconditioned by
131 passing 10 ml of sterile PBS. For each membrane filter type (i.e., coated with SWNT, PVK-
132 SWNT and non-coated), 2 ml of bacterial suspension in PBS at OD= 0.5 was passed through the
133 membrane filter. Each membrane filter was tested at least in duplicate.

134 2.6. Bacterial Viability Assay

135 This test was performed to determine the percentage of inactivated bacterial cells retained on
136 the surface of the membranes. The bacterial viability assay was performed using the
137 LIVE/DEAD BacLight kit (Invitrogen, USA) to quantify the number of live and dead cells on the
138 filter surfaces (Kang et al. 2008). Immediately after the filtrations, the filter surfaces were stained
139 with the LIVE/DEAD BacLight Bacterial Viability kit and were observed with a fluorescence
140 microscope (OLYMPUS, Japan). SYTO 9 dye was used to stain the total number of cells, while
141 propidium iodide (PI) was used to stain cells with compromised membranes. Five representative
142 images at 40x magnification were taken for each sample and all the samples were tested in
143 triplicate. Total cells and dead cells were counted with the Image-Pro Plus software
144 (MediaCybernetics, USA). The percent of inactivated cells was determined from the ratio of the
145 number of cells stained with PI divided by the number of cells stained with SYTO-9 plus PI. The
146 results were averaged out and the standard deviations were calculated.

147 *2.7. Bacterial quantification in the filtrate*

148 The plate count method was used to enumerate viable bacteria in the filtrate (Hilal et al.
149 2004). The filtrates were collected and diluted in PBS through serial dilution. The dilutions were
150 plated on Tryptic Soya Agar (TSA) (Oxoid, England) media and incubated overnight at 37⁰ C.
151 The total number of colony forming units (CFU) was enumerated. Each filtrate sample was
152 plated in duplicate and standard deviations were calculated from the results.

153 *2.8. Filter Agar test*

154 Viability and re-growth potential of the retained bacterial cells on the membrane surfaces were
155 tested using a previously described method (Hilal et al. 2004). Immediately after filtration, the
156 filter surfaces were flipped on a TSA plate facing down and incubated overnight at 37⁰ C.

157 Bacterial growth on the membrane perimeter was measured with a Mitutoyo 500-196-20 Digital
158 micrometer Caliper (MSI Viking Gage, USA). Averages and standard deviations were calculated
159 from triplicates.

160 *2.9. Scanning electron microscopy (SEM) Imaging*

161 SEM sample preparation and imaging was performed as previously described (Kang et al.
162 2007). Briefly, bacterial cells on the filter surfaces were fixed with 2% gluteraldehyde in 0.05M
163 cacodyle buffer solution (Fisher Scientific, USA). The fixed cells were subsequently stained with
164 1% osmium tetroxide (Sigma Aldrich Chemicals, USA) and dehydrated with increasing
165 concentrations of ethanol (25%, 50%, 75%, 95% and 100%). SEM images were acquired using a
166 LEO Gemini 1500 series microscope at 10 keV. Prior to imaging, the samples were mounted on
167 carbon tape and coated with Au/Pd using a Denton Vacuum Desk II sputter coater.

168 *2.10. Deoxyribonucleic acid (DNA) quantification assay*

169 This assay was performed to quantify the DNA concentration (ng/ μ l) in the filtrate that was
170 released from damaged bacterial cells after filtration. The experimental procedure was adapted
171 from a previously described method (Kang et al. 2008). Briefly, immediately after filtration, 2 μ l
172 of the filtrates were placed in a Take 3 Plate (for DNA quantification) in the Synergy MX
173 (BioTek, USA). Sterile PBS without bacteria and DNA were used as blanks. Average DNA
174 concentrations and standard deviations were calculated from duplicate filtrate samples.

175 *2.11. Viral culture and quantification*

176 MS2 bacteriophage was selected to test viral removal by these new membranes. MS2
177 bacteriophage and its host *E. coli* 15597 were obtained from the American Tissue Culture
178 Collection (ATCC). The stock solution of MS2 was prepared as previously described(Brady-

179 Estévez et al. 2010). Stock solutions of MS2 in PBS (4.5×10^{11} Plaque Forming Units (PFU)/ml)
180 were used for the filtration experiments. The concentrations of bacteriophages were determined
181 before and after each filtration experiment. The membrane filters were prepared and
182 preconditioned as described in *Section 2.5* “Bacteria Cell Filtration”. A solution of 2 ml of the
183 MS2 was filtered through the membrane filter at constant permeation rate ($\sim 57 \text{ L m}^{-2} \text{ h}^{-1}$). Filtrate
184 was collected on sterile 2 ml tubes and viral concentrations were determined with the PFU
185 method (Brady-Estévez et al. 2010). Briefly, each serial dilution in PBS of the filtrate was mixed
186 with the *E. coli* host and molten soft agar (0.7% TSA), then poured on TSA plates. The plates
187 were incubated overnight at 35°C and the plaque forming units were quantified. All the virus
188 experiments were done in a biological safety cabinet. Each filter was tested in duplicate and the
189 standard deviations were calculated.

190 191 *2.12. Cytotoxicity Evaluation*

192 Cytotoxicity test of PVK-SWNT, SWNT, and PVK solutions were performed against NIH
193 3T3 Fibroblast cells using CellTiter 96 AQueous (Promega) as previously described (Tria et al.
194 2010). The NIH 3T3 Fibroblasts were a gift from Dr. Albee Messing of the University of
195 Wisconsin-Madison and were cultured at 37°C in a growth media containing 86% of Dulbecco’s
196 modified Eagle’s medium, 10% fetal bovine serum (FBS), 1% penicillin-streptomycin, 1% 4-(2-
197 hydroxyethyl)-1-piperazineethanesulfonic acid in 1 M HEPES, 1% L-glutamine, and 1%
198 minimum essential medium (MEM) in 10 mM nonessential amino acids solution (100 \times ;
199 GibcoBRL). Fibroblast cells of passages 129 and 132 were harvested from culture flasks by 10-
200 12 min incubation with 0.25% trypsin and were resuspended in the growth media. Assay kits
201 containing 3- (4,5-dimethylthiazol-2-yl)-5-(3-carboxymethoxyphenyl)-2-(4-sulfophenyl)- 2H-
202 tetrazolium, inner salt (MTS) and an electron coupling reagent, phenazine methosulfate (PMS)

203 were used. Briefly, cells were seeded onto a 96-well plate with a seeding density of 2.5×10^4
204 cells/ 100 μ L and incubated at 37° C and 5% CO₂ in humidified air for 24 h. The cell culture
205 medium was then aspirated from the wells and the plates containing cells were gently rinsed with
206 Dulbecco's Modified Eagle Medium (DMEM) to remove any non-adherent cells. Next, 100 μ l of
207 nanomaterials (PVK, SWNT and PVK-SWNT) were added onto each well containing cells and
208 incubated for 24 h at 37° C with 5% CO₂. After the incubation, the nanomaterials dispersed in
209 solutions were aspirated and the wells were rinsed 3 times with DMEM. The adherent cells were
210 evaluated for their viability using MTS assay as described by the manufacturer (Promega,
211 Madison, WI, USA). Briefly, MTS and PMS detection reagents were mixed, using a ratio of
212 MTS/PMS 20:1. This procedure was done immediately before to addition to the cell culture
213 media (DMEM) in which a 1:5 ratio of detection reagents to cell culture medium was used. Then
214 the aspirated wells containing the samples were incubated for 2 h at 37 °C in a 5% CO₂
215 atmosphere. A well containing only the culture medium (i.e. DMEM) was used as a “medium
216 only” control. The untreated cell suspension was used as a negative control. For the positive
217 control, 4% paraformaldehyde in PBS buffer was added to the cells grown on the plate. The
218 absorbance of the formazan was read using a Synergy MX Microtiter plate reader (BioTek, VT)
219 at 495 nm.

220 **3. Results and Discussions**

221 *3.1. Filter membrane Characterization*

222 Prior to membrane fabrication, the PVK-SWNT and PVK sample solutions were
223 characterized using UV-Vis. Figure 1 shows the UV-visible spectra for the pure SWNTs. As
224 expected no absorption peaks at the visible region of the electro-magnetic spectrum were
225 observed. However for the pure PVK solution, main signature bands occurring at 331 and 345

226 nm were observed. These peaks are attributed to the π - π^* and n- π^* optical transitions in pendant
227 carbazole moieties of PVK (Fulghum et al. 2008). It can be seen from the spectra that the main
228 absorption peaks for pure PVK still prominent in the PVK-SWNT nanocomposite, but the
229 intensity was slightly reduced due to the presence of the SWNT. FTIR was also used to
230 determine the functional groups present on the modified filter surfaces. Figure 2 shows the IR
231 spectra of the nitrocellulose filter membrane with the following peak assignments: 832 cm^{-1} (NO
232 stretch), 1651 cm^{-1} (asymmetric NO_2 stretch), 1282 cm^{-1} (symmetric NO_2 stretch), 1060 cm^{-1}
233 (asymmetric CO stretch) and a weak band at 1746 cm^{-1} (CO stretch) (Sloane 1963). Similar
234 peaks were observed for the PVK-SWNT membranes corresponding to olefinic C-H bending
235 (822-837 cm^{-1}), C-N stretching (1012-1273 cm^{-1}) and C=C stretching (1635-1645 cm^{-1}), except
236 for the weak band at 1746 cm^{-1} found in bare nitrocellulose filter (inset). The disappearance of
237 this band as well as the significant increase of absorbance intensity in modified membranes
238 suggests successful coating of the filter with PVK-SWNT.

239 The successful modification of the filter was characterized using XPS (Figure 3). Narrow scan in
240 the N 1s region of the unmodified filter membrane showed an intense peak at ~408 eV coming
241 from N=O of the nitrocellulose membrane. Upon addition of PVK-SWNT, a new peak centered
242 at ~399 eV appeared, indicative of the N-C coming from the carbazole moieties of PVK.
243 Furthermore, the C 1s scan of the PVK-SWNT showed higher peak intensity in the C-C region
244 (284.5 eV) as compared to the PVK and unmodified membranes due to the incorporation of C-C
245 containing SWNT. To estimate the amount of SWNT loaded on the filter membrane, the peak
246 area ratios from the N-C and C-C peaks of the PVK-SWNT and PVK were used. Using this
247 method, the amount of SWNT was estimated to be ~3 wt %. This value is similar to the solution
248 mixture ratios of PVK-SWNT used to prepare the modified filter. The morphology of all the

249 membranes were evaluated using SEM. Figure 4a depicts the SEM image of the unmodified
250 nitrocellulose membrane, which revealed a layered and mat-like porous surface. The SWNT and
251 PVK-SWNT-modified filters, on the other hand, formed a denser coating on the surfaces that
252 were seen over several layers. Furthermore, the uniform aspect of the surfaces throughout the
253 membranes demonstrates successful and homogeneous coating of the nitrocellulose membrane
254 surfaces with SWNT and PVK-SWNT (Figure 4, b & c).

255 3.2. Antibacterial property of the coated membranes

256 The LIVE/DEAD assay was performed to determine bacterial viability after interaction with
257 the nanomaterials during filtration. Fluorescence microscopy was used to assess the loss of
258 bacterial viability. SYTO 9 dye (green dye) was used to stain both live and dead cells while
259 propidium iodide (PI) (red dye) was used stain the cells with compromised membranes. Figure 5
260 (a, b) shows representative fluorescence images of the *E. coli* and *B. subtilis* cells on the filter
261 surfaces. Results show that in the absence of the nanomaterials (control), bacterial inactivation
262 was <10% (Figure 5, c). While, ~90 % and ~81 % of the *E. coli* cells were inactivated after being
263 retained on the PVK-SWNT and SWNT coated membranes, respectively. Similarly, ~90 % and
264 ~40 % of the *B. subtilis* cells were inactivated after retained on PVK-SWNT and SWNT coated
265 membranes, respectively. In similar studies with SWNT coated membranes, 80-90 % *E coli*
266 inactivation was observed (Kang et al. 2007, Brady-Estévez et al. 2008). No noticeable toxicity
267 effects (inactivation < 10%) of PVK coated membranes were observed on either *E. coli* or *B.*
268 *subtilis*. This suggests that toxicity observed on PVK-SWNT coated membranes were either due
269 to the presence of SWNT or synergistic effects of PVK-SWNT, but not due to the presence of
270 PVK. In the case of 100% SWNT coated membranes (Figure 5, c), the toxic effect of these
271 membranes on *B. subtilis* were considerably smaller than on *E. coli*. However, these findings are

272 similar to many other studies where *E. coli* and *B. subtilis* exhibited different tolerance levels
273 towards SWNT. These finds were explained as differences in cell wall structure, the protective
274 effect of the outer membrane surface properties, ability to form spores and/or unique repair
275 mechanisms of different microorganisms (Aslan et al. 2010, Kang et al. 2009, Lyon and Alvarez
276 2008, Lyon et al. 2005).

277 The results demonstrated that PVK-SWNT nanocomposite with only 3% SWNT content
278 achieved similar or better cell inactivation than 100% SWNT coated membranes. These results
279 can be explained by the better dispersion and debundling of SWNT in the presence of PVK,
280 which would increase the probability of SWNT to be in contact with bacterial cells(Kang et al.
281 2007). Though the exact mechanism of SWNT-bacterial interaction has not been completely
282 elucidated yet, several studies suggested physical disruption of bacterial membrane and oxidative
283 stress as the major mechanisms (Aslan et al. 2010, Kang et al. 2007, Rodrigues and Elimelech
284 2010, Schiffman and Elimelech 2011). Therefore, the cells in contact with this nanomaterial
285 were probably inactivated by one or both mechanisms.

286 *3.3. Intracellular DNA Release*

287 Although the membrane damage test (LIVE-DEAD) is a strong indicator of cell damage,
288 not all damaged membranes will lead to bacterial cell death. Current literature describes that the
289 release of large quantities of intracellular material from cells, only occurs when bacterial cell
290 walls and cellular membranes suffer irreparable damages (Kang et al. 2008). In many SWNT
291 cytotoxicity studies, cell membrane damage has been reported as one of the mechanisms for
292 bacterial toxicity. This mechanism is verified by measuring the efflux of cytoplasmic material
293 (e.g. DNA) in the filtrate. In Figure 6, the filtration of both *E. coli* and *B. subtilis* yielded higher
294 DNA concentrations in the filtrate of SWNT and PVK-SWNT coated membranes than uncoated

295 and PVK coated membranes. In the case of SWNT coated membranes, ~2 fold and ~1 fold
296 increase in DNA efflux compared to the control were observed for *E. coli* and *B. subtilis*,
297 respectively. While for PVK-SWNT coated membranes, ~4 fold and ~2.5 fold increase in DNA
298 efflux were observed for *E. coli* and *B. subtilis*, respectively. In similar studies, release of
299 intercellular DNA was observed to be as high as 5 fold for *E. coli* as a result of the bacterial
300 interaction with SWNT and subsequent membrane damage (Kang et al. 2008, Kang et al. 2007).
301 In the case of PVK-SWNT coated membranes, the SWNTs were highly dispersed, which
302 increased the chances of cell interaction with the open ends of nanotubes and led to cellular
303 damage. Similar results were also described on studies with coated surfaces with SWNTs and
304 other polymers (Aslan et al. 2010, Ahmed et al. 2012, Schiffman and Elimelech 2011).

305 We believe that the measured DNA concentration in the filtrate of SWNT and PVK-SWNT
306 coated membranes should have been much higher than what we are reporting, since DNA tends
307 to adsorb to SWNT surfaces (Kang et al. 2008). This high efflux of DNA suggests considerable
308 bacterial cell membrane damage and potential cell death.

309 In Figure 7, the DNA efflux from *B. subtilis* cells (Gram-positive) was lower than from *E. coli*
310 cells (Gram-negative), which could be explained by the thicker peptidoglycan cell-wall found in
311 Gram-positive bacteria. This thick peptidoglycan cell-wall would make it harder for
312 nanomaterials to cause considerable cell membrane damage (Pratt and Kolter 1998, Yang et al.
313 2010).

314 *3.4. Filter Agar printing test*

315 Recent studies have shown that *E. coli* can endure and repair low to moderately damaged cell
316 membranes (Kang et al. 2008, García et al. 2006). The main goal of this test was to confirm the
317 results from the DNA release assay and determine at what extent the damaged bacterial cells

318 retained on the membrane filter could recover from the cellular damage and grow after the
319 exposure to the nanomaterial. In the results of the LIVE/DEAD and DNA release assays, the
320 control and PVK coated membrane filters presented very few bacterial cells with compromised
321 cellular membranes as opposed to SWNT and PVK-SWNT coated membrane filters. Similarly,
322 in the agar printing assay (Figure 7), much higher bacterial growth was observed on the control
323 and PVK-coated membranes than on the other coated membranes. SWNT membranes presented
324 ~73% and ~66% growth inhibition for *E. coli* and *B. subtilis*, respectively, when compared to the
325 control. Similar inhibition was also observed for PVK-SWNT membranes (~70% for *E. coli* and
326 ~65% for *B. subtilis*). These results suggest that bacteria retained on the membrane filters
327 significantly lose their potential for re-growth. Bacterial re-growth and biofilm formation have
328 been demonstrated in many studies to cause great problems in membrane operations (Zator et al.
329 2007); these results show that this new coating has the potential to solve such problems.

330 3.5. Bacterial morphology on the filters

331 The SEM images of *E. coli* (Figure 8) showed bacterial cells disrupted and shrunk on both
332 SWNT and PVK-SWNT filter surfaces. This result corroborates our results of the Live/Dead
333 assay, intracellular DNA release, and the filter agar printing test. Similar bacterial damage was
334 also observed for *B. subtilis* after filtration on the PVK-SWNT and SWNT modified
335 membranes.

336 3.6. Bacterial Removal Property

337 In theory, membrane filters with smaller pore size than the size of bacterial cells are
338 expected to retain all cells by a sieving mechanism. Studies, however, have shown that bacterial
339 cells can entrain through membrane pores due to high filtration rates, solution chemistry, and
340 lack of membrane surface uniformity (Brady-Estévez et al. 2010, Tufenkji and Elimelech 2003).

341 Our study demonstrated that both SWNT and PVK-SWNT coated filters had ~ 4 log higher
342 bacterial removal than the control filters (Figure 9). This bacterial removal might be a combined
343 effect of cell retention and inactivation by SWNT while passing through the membranes. The
344 small pore size (0.45 μm) of the nitrocellulose membranes, the added thickness of SWNT and
345 PVK-SWNT layers to the membrane, and the strong affinity of the bacterial cells to SWNT
346 surfaces increased the efficiency of the filters by cell inactivation, sieving, and depth filtration
347 mechanisms (Brady-Estévez et al. 2008, Brady-Estévez et al. 2010, Brady-Estévez et al. 2010).
348 The similar log removal of 100% SWNT coated membranes and PVK-SWNT coated membranes
349 with only 3% SWNT load could be attributed to a more homogeneous dispersion of SWNTs on
350 the membrane surface in the presence of PVK, and hence more SWNT open ends to inactivate
351 bacterial cells.

352 *3.7. Virus removal property*

353 MS2 bacteriophage was used to investigate the removal efficiency of nanometer-sized viral
354 particles. The bacteriophages were filtered through bare membranes (control), and through PVK,
355 SWNT, and PVK-SWNT coated membranes. As expected, the log removal of MS2 for both
356 control and PVK coated membranes were very poor (<1 log), due to the very small size of the
357 virus (~27-34 nm) compared to the membrane pore size (0.45 μm) (Figure 10). On the other
358 hand, the log viral removal was ~3 and ~2.2 for SWNT and PVK-SWNT coated membranes,
359 respectively. The mechanism of virus removal on SWNT coated membranes has been
360 demonstrated to be by depth filtration (Brady-Estévez et al. 2010). A higher virus removal (~3
361 logs) by 100% SWNT coated membranes than PVK-SWNT (with 3% of SWNT) coated
362 membranes can be attributed to a larger amount of SWNT in the 100% SWNT membranes. The
363 higher the SWNT concentration on the membrane, the larger will be the surface area available

364 for the virus particles to adsorb. Studies have shown that SWNT loads of 0.5 mg/cm² achieve
365 more than 4 log virus removal. Furthermore, a linear relationship was established between the
366 effluent virus concentration and SWNT load on the membrane surface (Brady-Estévez et al.
367 2010).

368 3.8. Cell cytotoxicity Test

369 During the filtration process, some SWNT particles may detach from the membrane surface and
370 end up in the drinking water. Certain concentrations of SWNTs have been shown to be toxic to
371 humans and other mammals. For instance, pure SWNT/MWNT was described to damage the
372 plasma membrane of mammalian cells and to induce considerable toxicity (Cheng et al. 2011,
373 Chen and Schluesener 2010). Therefore, it is essential to investigate the cytotoxicity of the SWNT
374 concentrations used in the filters in this study to assess their suitability for drinking water
375 treatment. Fibroblast cells are part of connective tissues and play an important role in wound
376 healing; therefore they are often used in *in vitro* studies. These cells can easily get exposed by
377 SWNT entering the mammalian cells through physical contact or ingestion (Tian et al. 2006).

378 The exposure of fibroblast cells to SWNTs showed that the concentration of SWNT plays an
379 important role in the toxic behavior of SWNT towards mammalian cells (Figure 11). In SWNT
380 samples, with a concentration of 1mg/ml, ~75% cytotoxicity was observed in the mammalian
381 cells. In the PVK-SWNT suspension with a SWNT concentration of 0.03 mg/ml was observed
382 only ~20% toxicity. PVK, on the other hand, that functions as dispersant, displayed minimal
383 cytotoxic effects (~10%). Previous studies with other mammalian cells, such as the human
384 umbilical vein endothelial cells, demonstrated that a SWNT mixture with the phosphorycholine
385 polymer exhibited a cytotoxicity of only ~8-10%, while SWNT/MWNT suspended with
386 polyethylene glycol (PEG) showed no considerable toxicity to mammalian cells (Yang et al.

387 2010, Cheng et al. 2011, Xu et al. 2008). The PEG and other polymers mixed with
388 SWNT/MWNT were reported to be able to penetrate mammalian cells without damaging the
389 plasma membrane, and their accumulation did not show significant toxic effect on cell cycle
390 (Chen and Schluesener 2010) . Hence, it seems that in the event of some leaching from the PVK-
391 SWNT coated membranes, the SWNT used in this study will not exhibit considerable toxicity
392 towards fibroblast cells. However, the effects of SWNT exposure to other mammalian cell types
393 and effects of chronic exposure need to be further investigated before such material can be
394 widely used for water treatment.

395 396 **4. Conclusion**

397
398 “In this study, we demonstrated that membrane (nitrocellulose) coated with SWNT and PVK-
399 SWNT nanocomposite can effectively remove and inactivate bacterial cells during filtration. The
400 PVK-SWNT (97:3 wt% ratio PVK: SWNT) coated membranes achieved similar or improved
401 bactericidal effects than 100% SWNT coated membrane. Log removal of MS2 virus was lower
402 in PVK-SWNT filters compared to 100% SWNT filters due to smaller loads of SWNT in the
403 nanocomposite, which reduced adsorption sites for the virus. The log removal efficiency (both
404 bacteria and virus) could be further investigated by increasing the thickness of PVK:SWNT and
405 SWNT coating. Again, substantial reduction of bacterial re-growth of the retained bacteria on the
406 new membranes and the high concentrations of intracellular material efflux (DNA, ng/ μ L) in the
407 filtrate are suggestive of irreversible bacterial cell membrane damage and bacterial death as a
408 possible mechanism of bacterial inactivation by both SWNT and PVK-SWNT membranes.
409 These observations are promising in terms of controlling biofouling problem during membrane
410 filter operations. Cytotoxicity tests on fibroblast cells demonstrated that PVK-SWNT (97:3 wt%
411 ratio PVK: SWNT) are considerably less toxic than pure SWNT (100%). Although SWNT and

412 PVK-SWNT membranes tested in this study showed impressive removal of pure bacterial
413 culture, further study should be conducted with natural water where many other factors like
414 natural organic material (NOM), complex microbial communities and solution chemistry can
415 influence the membrane filter performance.”

416 **Acknowledgements**

417 This research project was funded by the University of Houston New Faculty Research Program,
418 proposal # 102556 and by the NSF Research Experience for Teachers (RET) program (NSF
419 Award # 1130006). The authors would also like to thank Ms. Jennifer Dietz, Ms. Mady Landon,
420 and Mr. Yanni Economou for their assistance in performing the bacterial measurements. We are
421 grateful to Regina Aileen May V. Vergara and Maria Celeste R. Tria for their help in the
422 membrane preparation. We also would like to acknowledge Dr. Chellam for kindly providing the
423 MS-2 virus stock for this research.

426 **Supporting Information**

427 Additional data associated with this manuscript is provided in the Supporting Information
428 section.

429 **References**

- 430 Ahmed, F., Santos, C.M., Vergara, R.A.M.V., Tria, M.C.R., Advincula, R. and Rodrigues, D.F.
431 (2012) Antimicrobial Applications of Electroactive PVK-SWNT Nanocomposites.
432 *Environmental Science & Technology* 46(3), 1804-1810.
- 433 Ahuja, T., Mir, I., Kumar, D. and Rajesh (2007) Biomolecular immobilization on conducting
434 polymers for biosensing applications. *Biomaterials* 28(5), 791-805.
- 435 Arias, L.R. and Yang, L. (2009) Inactivation of Bacterial Pathogens by Carbon Nanotubes in
436 Suspensions. *Langmuir* 25(5), 3003-3012.
- 437 Aslan, S., Loebick, C.Z., Kang, S., Elimelech, M., Pfefferle, L.D. and Van Tassel, P.R. (2010)
438 Antimicrobial biomaterials based on carbon nanotubes dispersed in poly(lactic-co-glycolic acid).
439 *Nanoscale* 2(9), 1789.

440 Brady-Estévez, A.S., Kang, S. and Elimelech, M. (2008) A Single-Walled-Carbon-Nanotube
441 Filter for Removal of Viral and Bacterial Pathogens. *Small* 4(4), 481-484.

442 Brady-Estévez, A.S., Nguyen, T.H., Gutierrez, L. and Elimelech, M. (2010) Impact of solution
443 chemistry on viral removal by a single-walled carbon nanotube filter. *Water Research* 44(13),
444 3773-3780.

445 Brady-Estévez, A.S., Schnoor, M.H., Vecitis, C.D., Saleh, N.B. and Elimelech, M. (2010)
446 Multiwalled Carbon Nanotube Filter: Improving Viral Removal at Low Pressure. *Langmuir*
447 26(18), 14975-14982.

448 Chen, X. and Schluesener, H.J. (2010) Mode of dye loading affects staining outcomes of
449 fluorescent dyes in astrocytes exposed to multiwalled carbon nanotubes. *Carbon* 48(3), 730-743.

450 Cheng, J., Mezziani, M.J., Sun, Y.-P. and Cheng, S.H. (2011) Poly(ethylene glycol)-conjugated
451 multi-walled carbon nanotubes as an efficient drug carrier for overcoming multidrug resistance.
452 *Toxicology and Applied Pharmacology* 250(2), 184-193.

453 Cui, K.M., Tria, M.C., Pernites, R., Binag, C.A. and Advincula, R.C. (2011) PVK/MWNT
454 Electrodeposited Conjugated Polymer Network Nanocomposite Films. *ACS Applied Materials &*
455 *Interfaces* 3(7), 2300-2308.

456 Fulghum, T.M., Taranekekar, P. and Advincula, R.C. (2008) Grafting Hole-Transport Precursor
457 Polymer Brushes on ITO Electrodes: Surface-Initiated Polymerization and Conjugated Polymer
458 Network Formation of PVK. *Macromolecules* 41(15), 5681-5687.

459 García, D., Mañas, P., Gómez, N., Raso, J. and Pagán, R. (2006) Biosynthetic requirements for
460 the repair of sublethal membrane damage in *Escherichia coli* cells after pulsed electric fields.
461 *Journal of Applied Microbiology* 100(3), 428-435.

462 Guimard, N.K., Gomez, N. and Schmidt, C.E. (2007) Conducting polymers in biomedical
463 engineering. *Progress in Polymer Science* 32(8-9), 876-921.

464 Hilal, N., Kochkodan, V., Al-Khatib, L. and Levadna, T. (2004) Surface modified polymeric
465 membranes to reduce (bio)fouling: a microbiological study using *E. coli*. *Desalination* 167, 293-
466 300.

467 Kang, S., Herzberg, M., Rodrigues, D.F. and Elimelech, M. (2008) Antibacterial Effects of
468 Carbon Nanotubes: Size Does Matter! *Langmuir* 24(13), 6409-6413.

469 Kang, S., Mauter, M.S. and Elimelech, M. (2009) Microbial Cytotoxicity of Carbon-Based
470 Nanomaterials: Implications for River Water and Wastewater Effluent. *Environmental Science &*
471 *Technology* 43(7), 2648-2653.

472 Kang, S., Pinault, M., Pfefferle, L.D. and Elimelech, M. (2007) Single-Walled Carbon
473 Nanotubes Exhibit Strong Antimicrobial Activity. *Langmuir* 23(17), 8670-8673.

474 Khulbe, K.C., Matsuura, T., Singh, S., Lamarche, G. and Noh, S.H. (2000) Study on fouling of
475 ultrafiltration membrane by electron spin resonance. *Journal of Membrane Science* 167(2), 263-
476 273.

477 Liu, C.X., Zhang, D.R., He, Y., Zhao, X.S. and Bai, R. (2010) Modification of membrane
478 surface for anti-biofouling performance: Effect of anti-adhesion and anti-bacteria approaches.
479 *Journal of Membrane Science* 346(1), 121-130.

480 Lyon, D.Y. and Alvarez, P.J.J. (2008) Fullerene Water Suspension (nC60) Exerts Antibacterial
481 Effects via ROS-Independent Protein Oxidation. *Environmental Science & Technology* 42(21),
482 8127-8132.

483 Lyon, D.Y., Fortner, J.D., Sayes, C.M., Colvin, V.L. and Hughes, J.B. (2005) Bacterial cell
484 association and antimicrobial activity of a C60 water suspension. *Environmental Toxicology and*
485 *Chemistry* 24(11), 2757-2762.

486 Peng, F., Hu, C. and Jiang, Z. (2007) Novel ploy(vinyl alcohol)/carbon nanotube hybrid
487 membranes for pervaporation separation of benzene/cyclohexane mixtures. *Journal of Membrane*
488 *Science* 297(1-2), 236-242.

489 Pratt, L.A. and Kolter, R. (1998) Genetic analysis of *Escherichia coli* biofilm formation: roles of
490 flagella, motility, chemotaxis and type I pili. *Molecular Microbiology* 30(2), 285-293.

491 Rodrigues, D.F. and Elimelech, M. (2010) Toxic Effects of Single-Walled Carbon Nanotubes in
492 the Development of *E. coli* Biofilm. *Environmental Science & Technology* 44(12), 4583-4589.

493 Schiffman, J.D. and Elimelech, M. (2011) Antibacterial Activity of Electrospun Polymer Mats
494 with Incorporated Narrow Diameter Single-Walled Carbon Nanotubes. *ACS Applied Materials*
495 *& Interfaces* 3(2), 462-468.

496 Sloane, H. (1963) Infrared Differential Technique Employing Membrane Filters. *Analytical*
497 *Chemistry* 35, 1556-1558.

498 Tian, F., Cui, D., Schwarz, H., Estrada, G.G. and Kobayashi, H. (2006) Cytotoxicity of single-
499 wall carbon nanotubes on human fibroblasts. *Toxicology in Vitro* 20(7), 1202-1212.

500 Tria, M.C.R., Grande, C.D.T., Ponnampati, R.R. and Advincula, R.C. (2010) Electrochemical
501 Deposition and Surface-Initiated RAFT Polymerization: Protein and Cell-Resistant
502 PPEGMEMA Polymer Brushes. *Biomacromolecules* 11(12), 3422-3431.

503 Tufenkji, N. and Elimelech, M. (2003) Correlation Equation for Predicting Single-Collector
504 Efficiency in Physicochemical Filtration in Saturated Porous Media. *Environmental Science &*
505 *Technology* 38(2), 529-536.

506 Upadhyayula, V.K.K. and Gadhamshetty, V. (2010) Appreciating the role of carbon nanotube
507 composites in preventing biofouling and promoting biofilms on material surfaces in
508 environmental engineering: A review. *Biotechnology Advances* 28(6), 802-816.

509 Xu, F.-M., Xu, J.-P., Ji, J. and Shen, J.-C. (2008) A novel biomimetic polymer as amphiphilic
510 surfactant for soluble and biocompatible carbon nanotubes (CNTs). *Colloids and Surfaces B:*
511 *Biointerfaces* 67(1), 67-72.

512 Yang, C., Mamouni, J., Tang, Y. and Yang, L. (2010) Antimicrobial Activity of Single-Walled
513 Carbon Nanotubes: Length Effect. *Langmuir* 26(20), 16013-16019.

514 Zator, M., Ferrando, M., López, F. and Güell, C. (2007) Membrane fouling characterization by
515 confocal microscopy during filtration of BSA/dextran mixtures. *Journal of Membrane Science*
516 301(1–2), 57-66.

517

Figure File

(Antimicrobial PVK:SWNT nanocomposite coated membrane for water purification: performance and toxicity testing)

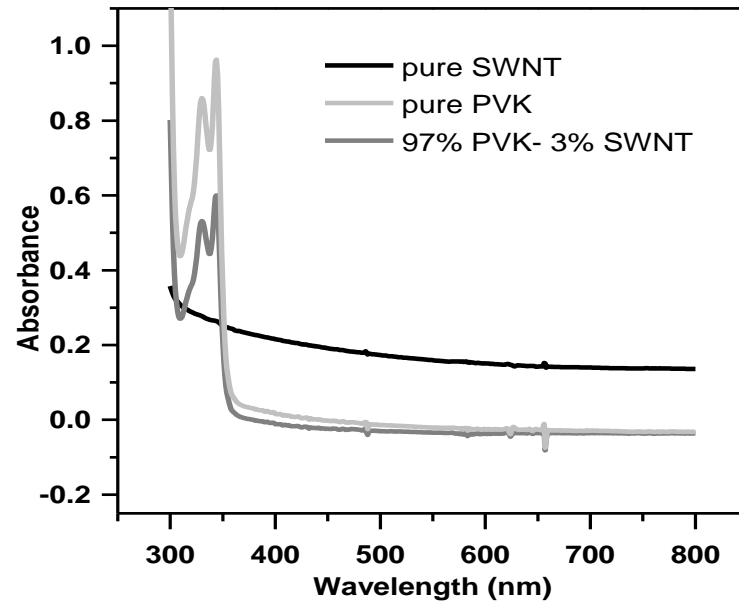


Figure 1. UV-vis spectra of the pure SWNT, PVK and PVK-SWNT nanocomposite solutions.

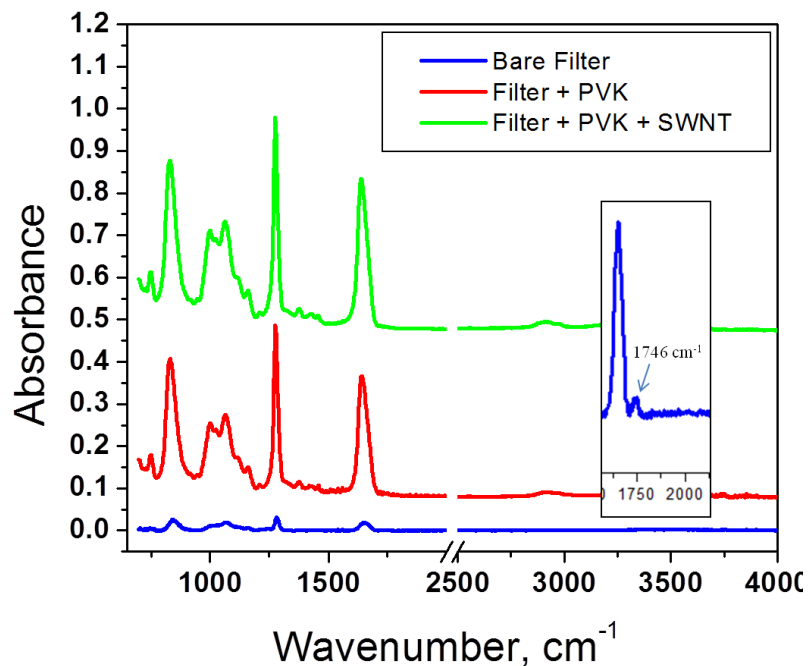


Figure 2. FTIR spectra of the unmodified, PVK-modified and PVK-SWNT modified nitrocellulose membranes.

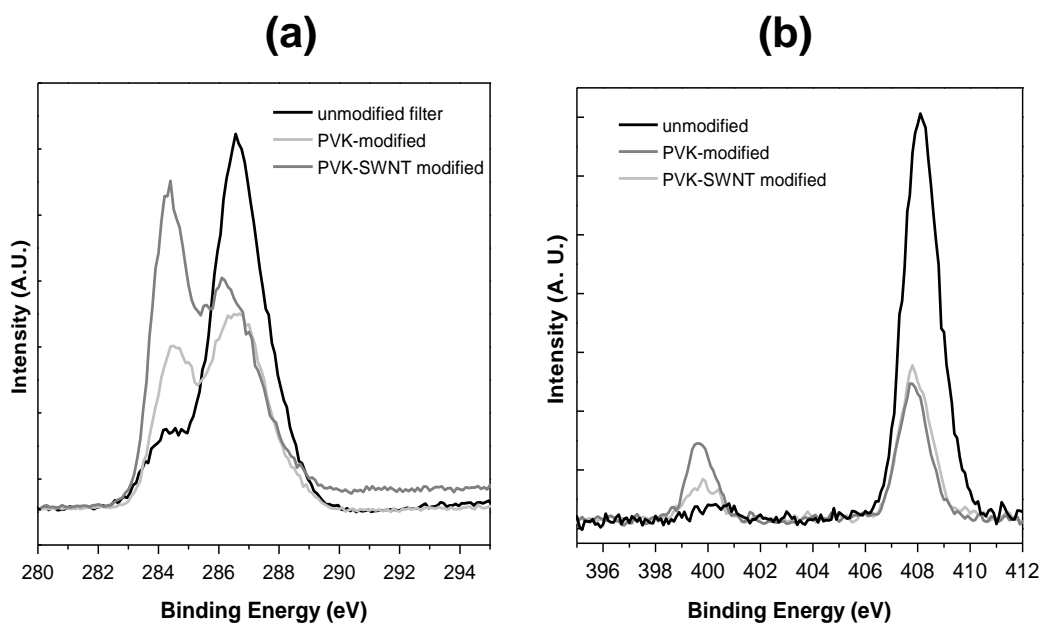


Figure 3. XPS spectra of the unmodified, PVK-modified, and PVK-SWNT modified nitrocellulose membrane. (a) C 1s and (b) N 1s regions.

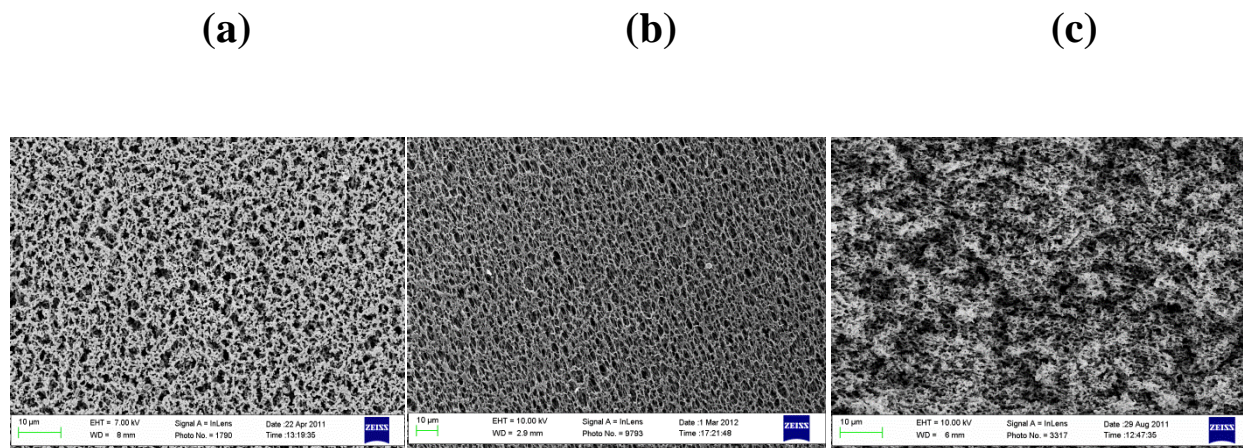


Figure 4. SEM images of membrane morphologies: (a) bare nitrocellulose membrane; (b) SWNT coated membrane; (c) PVK-SWNT coated membrane. Scale: 10 μm

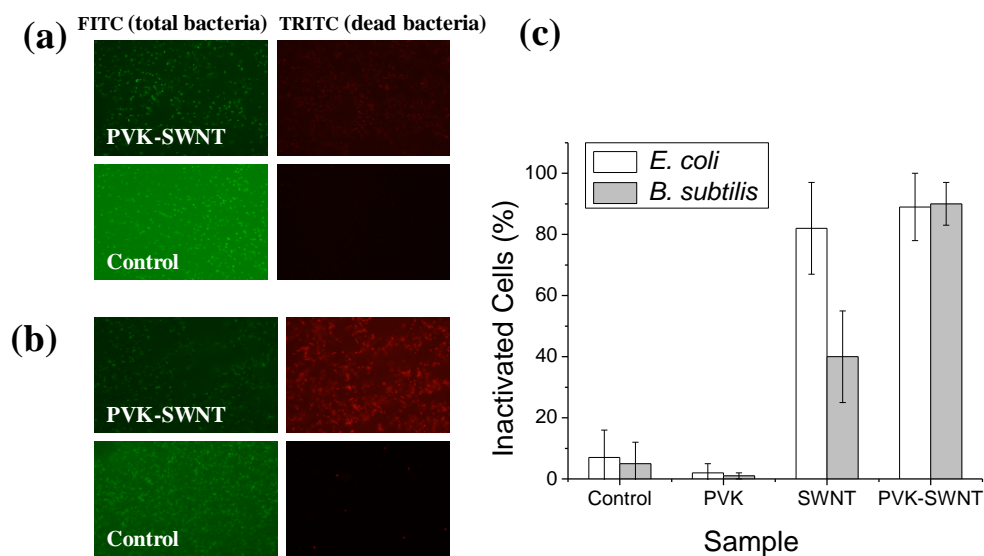


Figure 5. Viability assay for bacteria retained on membrane filters: (a) representative digital images after live and dead cell staining of *E. coli* retained on PVK-SWNT coated filter and on bare filter (control); (b) representative digital images after live and dead cell staining of *B. subtilis*.

subtilis retained on PVK-SWNT coated filter and on bare filter (control). (c) Correlation of the % of non-viable *E. coli* and *B. subtilis* (percent inactivated cells) after retention on PVK-SWNT, SWNT, PVK and bare filters.

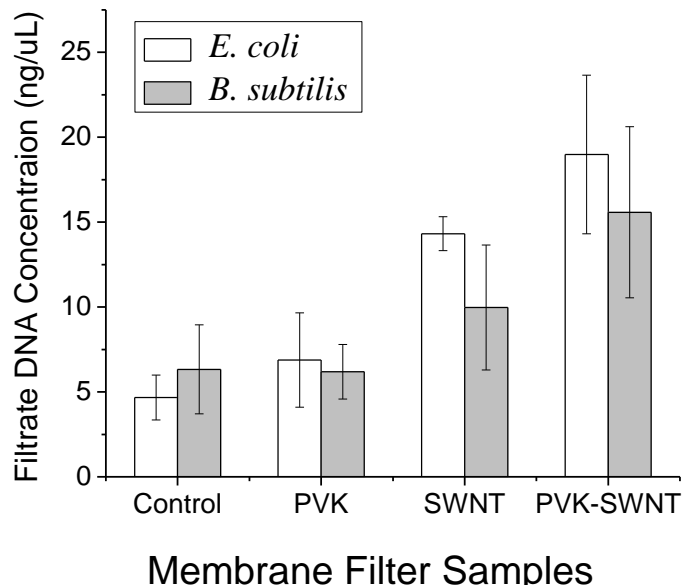


Figure 6. Efflux of cytoplasmic material (DNA, ng/μL) in the filtrate after filtration of *E. coli* and *B. subtilis* through PVK, SWNT and PVK-SWNT coated membrane filter and non-coated filter (control).

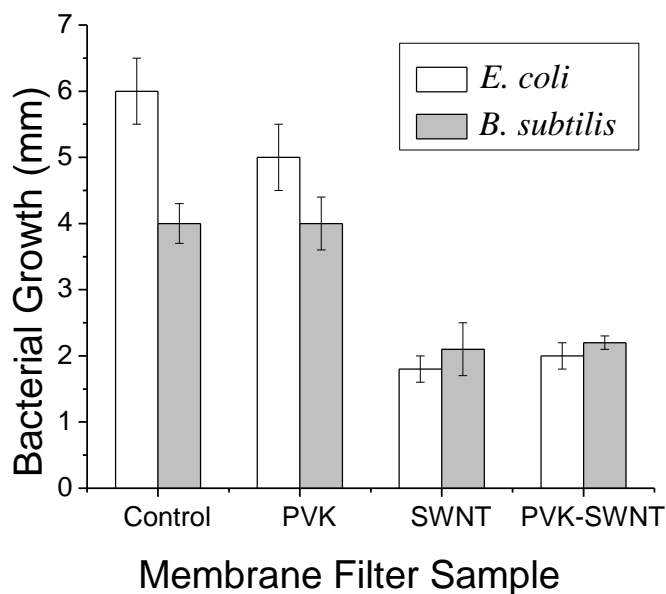


Figure 7. Agar printing assay to determine the growth behavior of bacteria retained on membrane coated with PVK, SWNT, PVK-SWNT and bare membrane (Control).

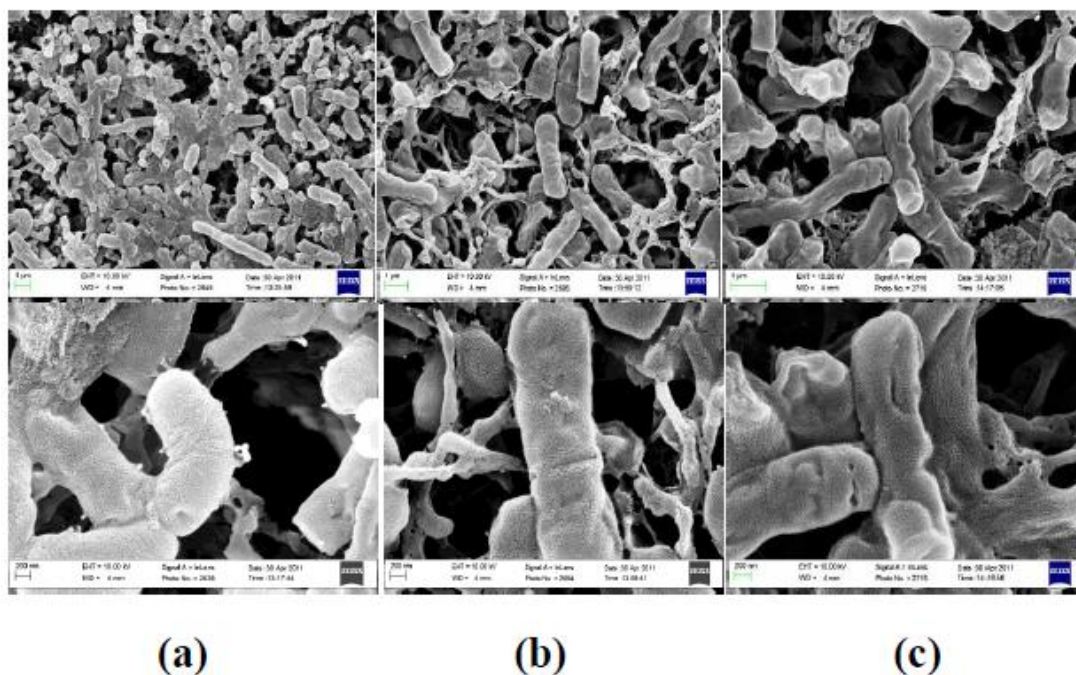


Figure 8. SEM images of membrane filter with retained bacterial (*E. coli*) cells on (a) unmodified membrane (control), (b) SWNT coated membrane, and (c) PVK-SWNT coated membrane. Scale: 1 μm (top), 200 μm (bottom).

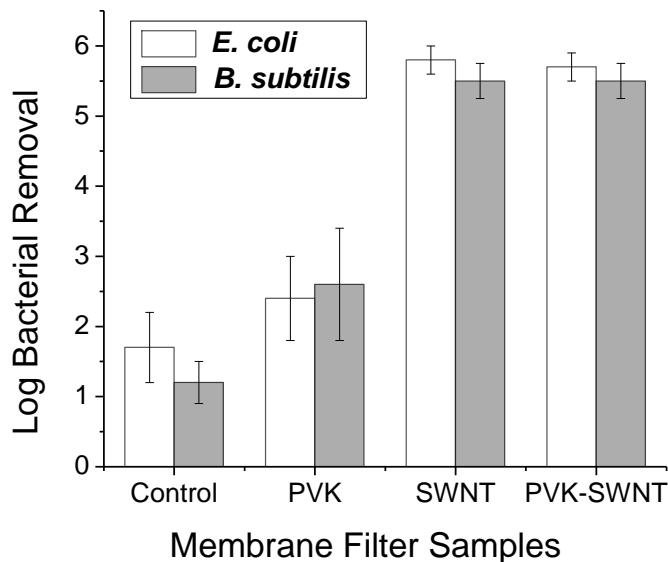


Figure 9. *E. coli* and *B. subtilis* (10^7 CFU/ml) log removal after filtration at constant permeation rate through bare membrane (control) and through PVK, SWNT and PVK-SWNT coated membranes.

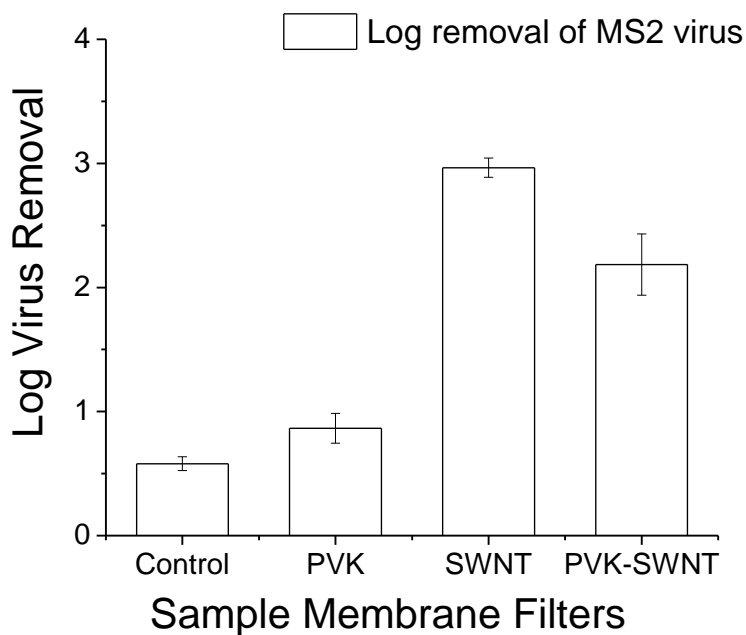


Figure 10. Log removal of MS2 virus (4.5×10^{11} PFU/ml) after filtration at constant permeation rate through bare membrane (control) and through PVK, SWNT, and PVK-SWNT coated membranes.

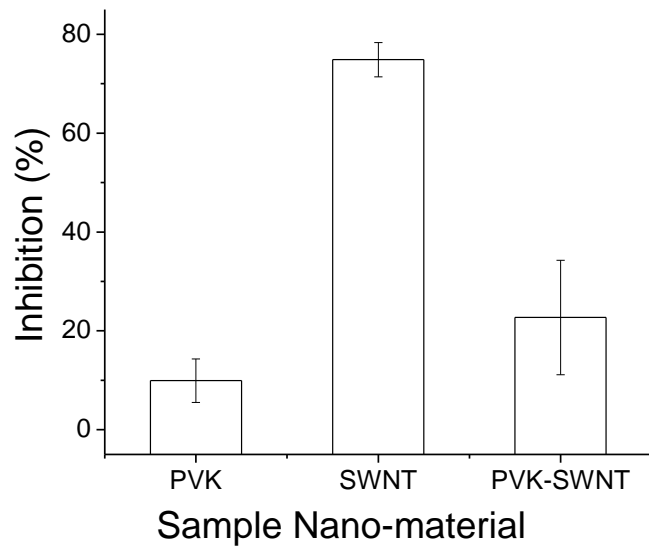


Figure 11. Cytotoxicity of the PVK-SWNT (1000 $\mu\text{g/ml}$), SWNT (1000 $\mu\text{g/ml}$), and PVK (1000 $\mu\text{g/ml}$) solutions against NIH-3T3 Fibroblasts.

Figure file (Supporting Information)

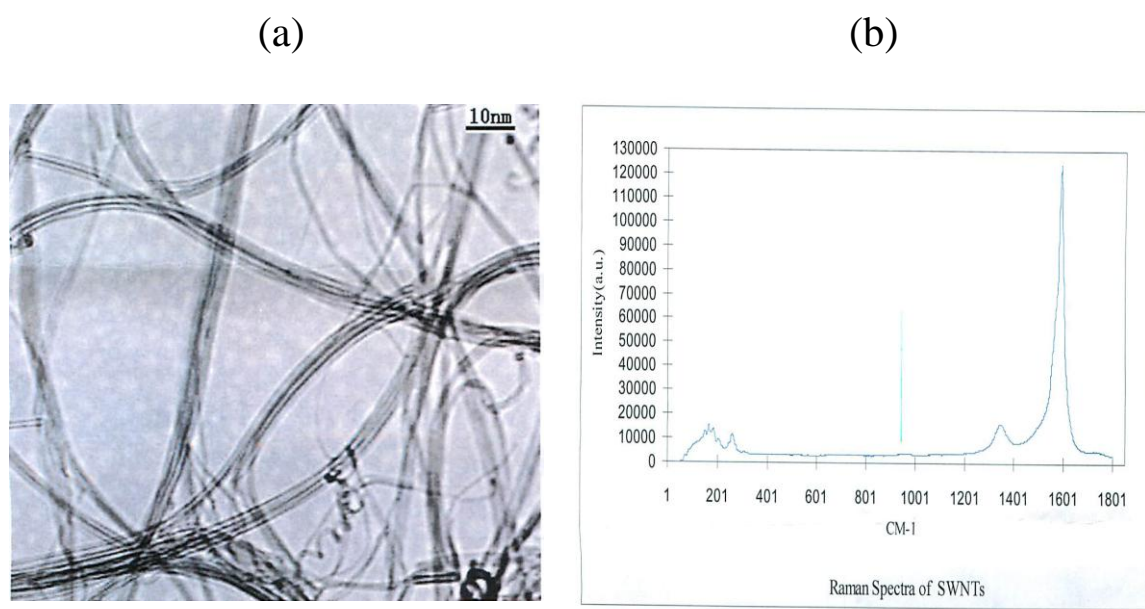


Figure S1. (a) Transmission Electron Microscopy (TEM) image (b) Raman spectra of SWNT supplied by the manufacturer (Cheap Tubes, VT)

Electronic Supplementary Material (for online publication only)

[Click here to download Electronic Supplementary Material \(for online publication only\): Supporting Info.doc](#)